

# **Numerical Simulation of Wave Interaction with Horizontal Slotted Submerged Breakwater**

Rounak Afroz<sup>1</sup>, and Md. Aatur Rahman<sup>2</sup>

*In this research work the interaction between waves and horizontal slotted submerged breakwater has been investigated using numerical model. Two-dimensional numerical model based on the SOLA-VOF (SOLution Algorithm-Volume Of Fluid) method developed for wave interaction with fixed submerged breakwater has been updated in this research to study the wave interaction with horizontal slotted submerged breakwater. From the developed two-dimensional numerical model water surface profile, velocity components, magnitude of pressure around breakwater of different porosities ( $n=0.4, 0.5$  and  $0.6$ ) and the value of  $F$  (VOF function) that represents fraction of volume occupied by fluid at any time are obtained. This study is expected to serve as a useful model to analyze wave deformation due to horizontal slotted submerged breakwater and will be important for designing submerged porous breakwater as a coastal protection measure.*

**Keywords:** Horizontal slotted, submerged breakwater, SOLA-VOF

## **1. Introduction**

Breakwaters have traditionally been used only for harbor protection and navigational purposes; but in recent years, designs of shore-parallel segmented breakwaters have been used for shore protection purposes. Segmented breakwaters can be used to provide protection over longer sections of shoreline. Wave energy is able to pass through the breakwater gaps, allowing for the maintenance of some level of longshore sediment transport, as well as mixing and flushing of the sheltered waters behind the structures. Various aspects of two and three dimensional problems of wave interaction with submerged, bottom founded, or floating surface-piercing structures have been studied numerically by many investigators. Wu et al (2012) studied the interactions between a non-breaking solitary wave and a submerged permeable breakwater experimentally and numerically. Balaji (2012) studied the hydrodynamic performance of porous breakwater by numerical analysis to assess reflection and transmission characteristics. Al-Banna and Liu (2007) conducted a numerical study on the hydraulic performance of submerged porous breakwater under solitary wave attack based on solving the Reynolds-Averaged Navier-Stokes (RANS) equations. Rahman and Womera (2013) investigated the interaction between waves and rectangular submerged impermeable breakwater. To predict the investigation, a two-dimensional numerical model based on the SOLA-VOF method was proposed there.

---

<sup>1</sup>Assistant Professor, Dept. of Water Resources Engineering, BUET, Email: rounak@wre.buet.ac.bd

<sup>2</sup> Professor, Dept. of Water Resources Engineering, BUET, Email: mataur@wre.buet.ac.bd

In this study the two-dimensional model of wave interaction with fixed submerged breakwater developed by Rahman and Womera (2013) is updated to adapt it for simulating wave interaction with horizontal slotted submerged porous breakwater. Here the structure has been made permeable by slotting the structure and measure the energy dissipation by breaking waves.

After describing the background section in the introduction, section 2 focuses on the computational procedure of the numerical model and then results and discussion in section 3 with the conclusion in section 4.

## 2. Numerical Model Based On SOLA-VOF

### 2.1 Basic Equations

The basic equations used for VOF method are the continuity equation, the Navier-Stokes equation for incompressible fluid and the advection equation that represents the behavior of the free surface. Because the wave generation source is placed within the computational domain, these equations involve the wave generation source. The continuity equation is,

$$\frac{\partial u}{\partial x} + \frac{\partial w}{\partial z} = q(x, z, t) \quad (1)$$

$$q(x, z, t) = \begin{cases} q^*(z, t); & x = x_s \\ 0; & x \neq x_s \end{cases} \quad (2)$$

where  $u$  and  $w$  are the flow velocity of  $x$  and  $z$  direction respectively,  $q$  is the wave generation source with  $q^*$  as the source strength which is only located at  $x = x_s$  and  $t$  is the time. The wave generation source  $q^*$  is defined as follows so that the vertically integrated quantity of  $q^*$  is equal to that in the non-reflection case (Ohyama and Nadaoka, 1991).

$q^*$  is also gradually intensified for the three wave periods from the start of wave generation in order to guarantee a stable regular wave train, as mentioned by Brorsen and Larsen (1987), shown in Equation 3.

$$q^* = \begin{cases} \left\{ 1 - \exp\left(-\frac{2t}{T_i}\right) \right\} 2U_0 \frac{\eta_0 + h}{\eta_0 + h} / \Delta x_s & : t/T_i \leq 3 \\ 2U_0 \frac{\eta_0 + h}{\eta_0 + h} / \Delta x_s & : t/T_i > 3 \end{cases} \quad (3)$$

where  $t$  is the time from the start of wave generation,  $T_i$  is the incident wave period,  $h$  is the still water depth, and  $\eta_s$  is the water surface elevation at the source line ( $x = x_s = 0$ ).  $\Delta x_s$  is the mesh size in the  $x$ -direction at  $x = x_s$ , and is required in order to apply the non-reflective wave generator to the finite difference method.  $U_0$  and  $\eta_0$  are the time variation of horizontal velocity and water surface based on third-order Stokes wave

## Afroz & Rahman

theory, respectively. The coefficient "2" of  $U_0$  in the right hand side of Equation 3 corresponds to two propagating waves toward both the left and right sides of the wave generation source. The Navier-Stokes equation,

$$\frac{\partial u}{\partial t} + u \frac{\partial u}{\partial x} + w \frac{\partial u}{\partial z} = -\frac{1}{\rho} \frac{\partial p}{\partial x} + \nu \left( \frac{\partial^2 u}{\partial x^2} + \frac{\partial^2 u}{\partial z^2} \right) + uq \quad (4)$$

$$\frac{\partial w}{\partial t} + u \frac{\partial w}{\partial x} + w \frac{\partial w}{\partial z} = -\frac{1}{\rho} \frac{\partial p}{\partial z} + \nu \left( \frac{\partial^2 w}{\partial x^2} + \frac{\partial^2 w}{\partial z^2} \right) + wq + \frac{1}{3} \nu \frac{\partial q}{\partial z} - g - \beta w \quad (5)$$

where  $p$  is the pressure,  $\nu$  is the kinematic viscosity,  $\rho$  is the fluid density,  $g$  is the gravitational acceleration and  $\beta$  is the wave dissipation factor which equals 0 except for the added dissipation zone. The advection equation of VOF function  $F$  is derived by considering conservation of mass of the fluid in each cell. The advection equation of VOF function  $F$  is,

$$\frac{\partial F}{\partial t} + \frac{\partial uF}{\partial x} + \frac{\partial wF}{\partial z} = Fq \quad (6)$$

### 2.2 Computational Procedure

**Figure1: Free Surface Geometric Model of VOF Method for Porous Breakwater**

	E	E	E	E	E	E	E	E	E	E	E	E	E	E
	E	E	E	E	E	S	S	S	S	S	S	S	E	E
	S	S	E	E	S	S	F	F	F	F	F	S	S	S
	F	S	S	S	S	F	OB	OB	OB	F	F	F	F	F
	F	F	F	F	F	F	F	F	F	F	F	F	F	F
	F	F	F	F	F	F	OB	OB	OB	F	F	F	F	F
	F	F	F	F	F	F	F	F	F	F	F	F	F	F
	F	F	F	F	F	F	OB	OB	OB	F	F	F	F	F

E = Empty cell, S = Surface cell, F = Fluid cell, OB= Obstacle cell

equations (1) to (6) are calculated by a finite difference method using staggered mesh. The free surface geometric model of VOF method for porous breakwater is shown in figure 1. The grid size of 2 cm in the x direction and 1cm in the z direction has been used in the model. On the staggered mesh, the flow velocities  $u$  and  $w$  are put on the cell boundary, and the pressure  $p$ , wave generation source  $q$  and VOF function  $F$  are set on the center of each cell. The cell is classified into four types; a full cell filled with fluid, an empty cell occupied by air, a surface cell containing both fluid and air and an obstacle cell that represents the structure. The SOLA scheme is employed to calculate

## Afroz & Rahman

the pressure and flow velocity in each time step. And a type of donor-acceptor flux approximation is used to calculate the advection of the VOF function  $F$  computing the free surface. The advectons are calculated by velocities of the adjoining cell using a donor cell which transports a fluid and an acceptor cell which receives the advect fluid. The physical characteristics of the cell are defined by the values of VOF function  $F$ . The cell in air, in the surface and in the water are denoted with  $F=0$ ,  $0<F<1$ , and  $F=1$  respectively.

### 2.3 Boundary Conditions

There are two boundary conditions for water particle velocity, that is, a boundary condition for the velocity parallel to the free-surface and a boundary condition for the velocity normal to the free-surface. In the first boundary condition the velocity on the surface cell is set equal to the velocity on the interface in contact with the adjacent full cell, which can be calculated by the governing equations. In the second boundary condition, the velocity is determined so that the continuity equation is satisfied in surface cells. The linear interpolation or extrapolation between the pressure on the free surface (atmospheric pressure) and the pressure of the adjacent full cell is used to calculate the pressure of the surface cell. An added dissipation zone method (Hinatsu, 1992) is used to treat the open boundaries. The waves are damped by numerical dissipation effects due to the coarse grids and the fictitious damping forces based on the Stokes damping law. Sommerfeld radiation condition is applied for the open boundaries. And, non-slip condition is applied on the sea bed. To adapt the model for horizontal slotted submerged breakwater, the boundary condition at the obstacle location is changed. The width of the obstacle is kept fixed and in vertical direction obstacle cells are declared keeping gaps for the fluid cells to flow between the obstacle cells as all the cells in the computational domain were declared as fluid cells earlier. And in the obstacle faces no slip condition is applied.

### 2.4 Numerical Model Run Conditions

At first, the developed numerical model is run for incident wave period,  $T= 1.6$  sec, incident wave height,  $H_i=12$  cm and  $h=50$  cm without any breakwater in the computational domain. The model simulated water surface profiles are compared with the waves generated from Stokes 3<sup>rd</sup> order wave theory. Then the model is run for different wave periods ranging from 1.6 sec to 2.0 sec for breakwaters of three different porosities as  $n=0.4$ , 0.5 and 0.6 to simulate water surface profile, velocity profile, VOF function  $F$  and pressure along the computational domain. Table 1 shows typical inputs in the numerical model and Table 2 shows the incident wave property for different run conditions.

## Afroz & Rahman

**Table 1: Typical Inputs in the Numerical Model**

X axis length		800 cm
Z axis length		74 cm
Structure position (from source)		400 cm
Still water depth		50 cm
Structure dimension	Width along wave direction	100 cm
	Length normal to wave direction	76 cm
	Height	40 cm

**Table 2: Incident Wave Property for Different Run Conditions**

Run No.	Incident Wave Height	Incident Wave Period	Porosity
Run 1	12	1.6	0.4
Run 2	13	1.7	0.4
Run 3	14	1.8	0.4
Run 4	15	2.0	0.4
Run 5	12	1.6	0.5
Run 6	13	1.7	0.5
Run 7	14	1.8	0.5
Run 8	15	2.0	0.5
Run 9	12	1.6	0.6
Run 10	13	1.7	0.6
Run 11	14	1.8	0.6
Run 12	15	2.0	0.6

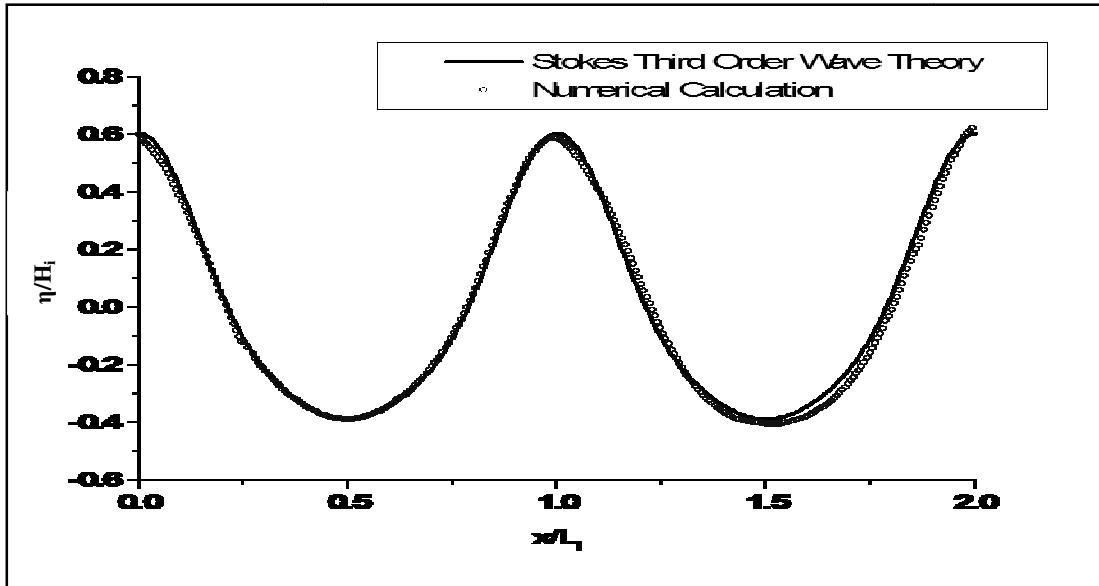
### 3. Results and Discussions

#### 3.1 Verification of the Numerical Model

At first, the developed numerical model is run for incident wave period,  $T= 1.6$  sec, incident wave height,  $H_i=12$  cm and  $h=50$  cm without any breakwater in the computational domain. The model simulated water surface profiles are compared with the waves generated from Stokes 3<sup>rd</sup> order wave theory. Then the model is run for different wave periods ranging from 1.6 sec to 2.0 sec for breakwaters of three different porosities as  $n=0.4$ , 0.5 and 0.6 to simulate water surface profile, velocity profile, VOF function  $F$  and pressure along the computational domain.

Wave generated by the developed model show good agreement with the wave generated by Stokes 3<sup>rd</sup> order wave theory which is displayed in Figure 7.

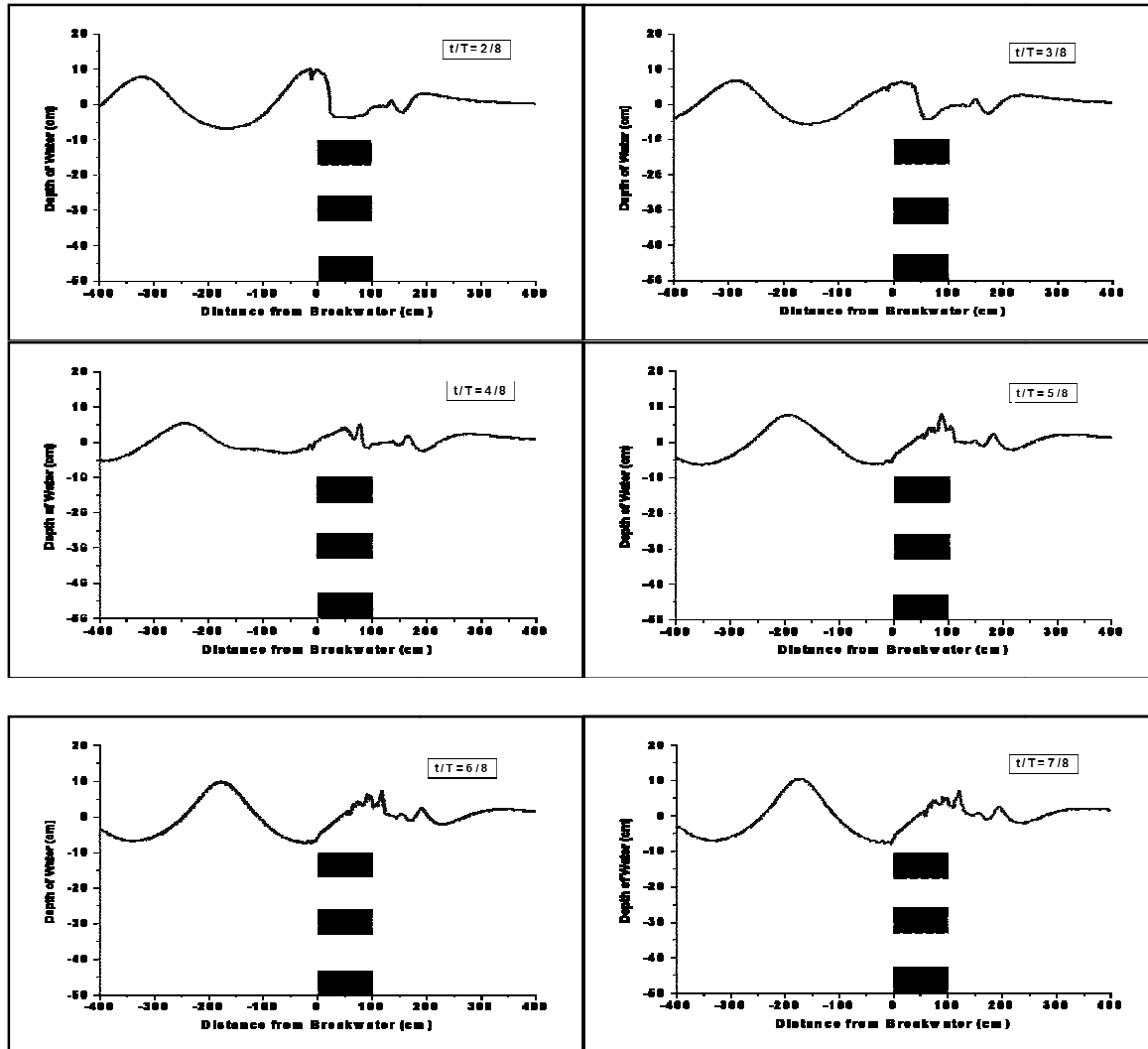
Figure 2: Comparison of Dimensionless Water Surface Profiles by Numerical Computation and 3<sup>rd</sup>-Order Stokes Wave Theory ( $H_i=12\text{cm}$ ,  $T=1.6\text{ Sec}$ ,  $H=50\text{ Cm}$ )



### 3.2 Numerical Model Simulation of Time Series Water Surface Profiles

Figure 3 shows the numerical simulation of water surface profiles along the flume length for different stages of a wave cycle. The wave height, the wave period and the water depth are considered as 12 cm, 1.6 seconds and 50 cm respectively. The depth and width of the submerged body are 40 cm and 100 cm respectively. The water surface profiles at different moments of a full wave period ( $T$ ) are shown in the figure. The overtopping of the water surface over the submerged body is seen in the figure. The irregular water surface profiles just behind the breakwater indicate the wave breaking and after breaking it is seen that the wave height reduces. Since the model is able to express the overtopping, the model can calculate the wave deformation around the structure due to nonlinear effects.

Figure 3: Numerical Model Simulation of Time Series Water Surface Profile for Run 1



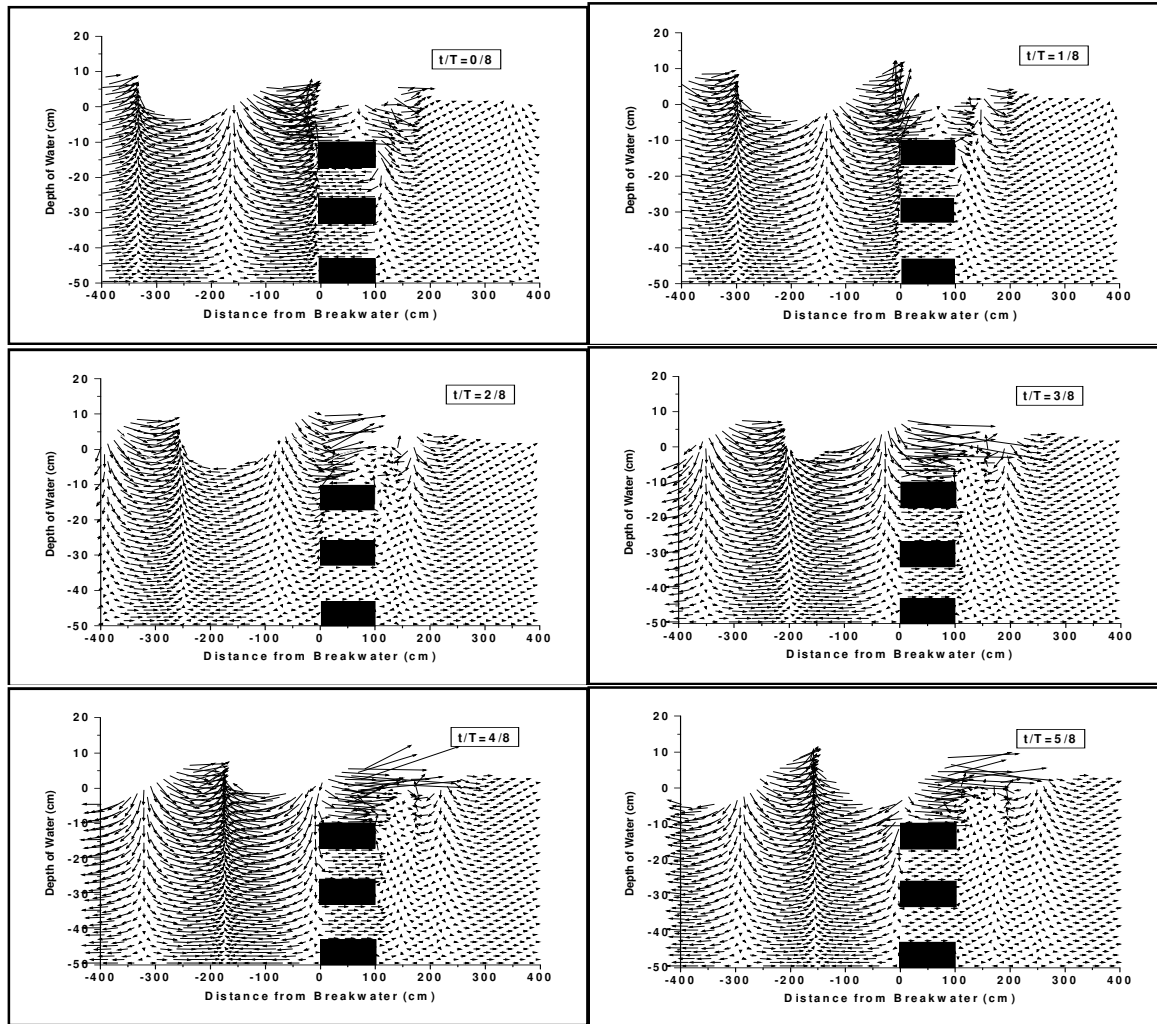
### 3.3 Numerical Model Simulation of Point Velocity around the Breakwater

The water particle velocity field around the breakwater at the moment of  $t=5.0$  second after starting the simulation is shown in Figure 4. The wave height, the wave period and the water depth are considered as 12 cm, 1.6 seconds and 50 cm respectively. The details of numerical simulation of the water particle velocity field around the breakwater for different stages of a wave cycle are shown.

From the Figure 4, it is seen that the vortexes are generating behind the breakwater and the wave passing over the breakwater breaks with an overturning wave front. The arrow of the vector represents the direction and the length of arrow represents the magnitude of the velocity. Furthermore, this figure illustrates that the higher magnitude of the water particle velocity in the offshore side of the breakwater decreases in the onshore side due to the wave energy dissipation through wave breaking by the breakwater. Also the

greater length of arrows over or just behind the breakwater shows breaking of waves in that zone.

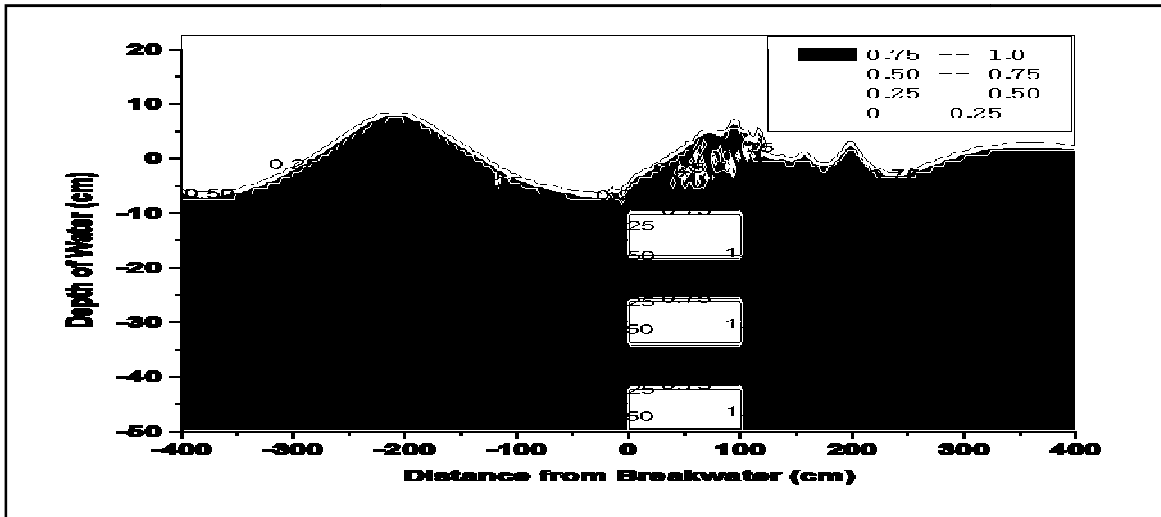
**Figure 4: Numerical Model Simulation of Time Series Water Particle Velocity Around the Horizontal Slotted Submerged Breakwater for Run 1**



### 3.4 VOF Function F around the Breakwater

Figure 5 shows the numerical simulation of the contour map of the VOF function  $F$ , which ranges from 0 to 1 at the moment of  $t = 6$  sec after starting the simulation. The wave height, the wave period and the water depth are considered as 13 cm, 1.7 seconds and 50 cm respectively.

Figure5: Numerical Model Results of VOF Function Value F Around the Breakwater

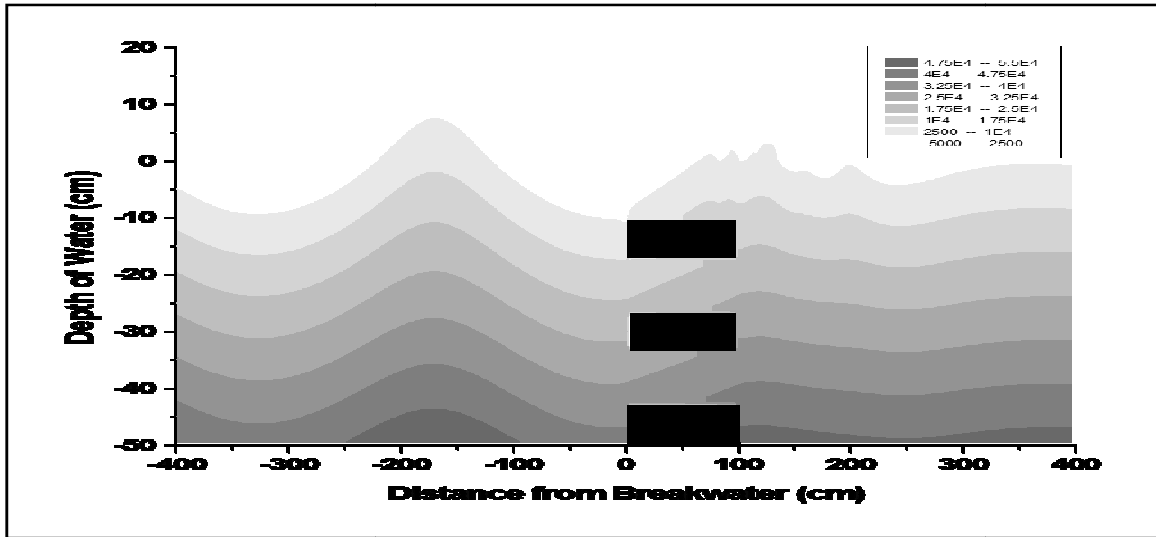


In Figure 5, the  $F$  value of the top surface of the water surface profile is seen less than 1 ( $F < 1$ ), that represents the surface cells. It shows that the breaking of wave occurs here and the air-bubble entrained in the corresponding numerical mesh cells due to wave breaking reduces the water volume less than the full volume of a fluid cell. For this reason the numerical model calculates  $F$  value of these cells less than 1. Also, the cells having  $F < 1$  are seen in offshore side of the breakwater. This may happen due to the reason that the higher water particle velocity in vertically downward direction at the offshore face of the breakwater may cause partial void at some cells near the offshore face bottom corner forming vortex in this zone.

### 3.5 Pressure Distribution Around the Breakwater

Figure6 shows the numerical simulation of the water pressure distribution ( $n=.04$ ) at the moment of  $t = 6$  sec after starting the simulation in  $\text{dyne/cm}^2$  unit. The wave height, the wave period and the water depth are considered as 12 cm, 1.6 seconds and 50 cm respectively. The solid portion in the middle of this figure represents the breakwater. The changes in the pressure distribution around the breakwater are presented here.

Figure 6: Numerical Model Results of Pressure Distribution Around the Breakwater for Run 1



#### 4. Conclusions

Horizontal slotted submerged porous breakwater is able to enhance water circulation and exchange of water between the open sea and sheltered areas. Because of the submergence of the breakwater, its application of protecting coastal areas attracts more attention due to environmental concerns. A two-dimensional numerical model of wave interaction with submerged solid breakwater developed by Rahman and Womera (2013) is adapted in this study to simulate the wave interaction with horizontal slotted submerged breakwater. The adapted model can simulate water surface profile, velocity profile, water pressure all through the flume length including wave breaking over and around the breakwater. From this study it is found that the water surface profiles simulated by the numerical model are in good agreement with wave profiles generated from Stokes 3<sup>rd</sup> order wave theory which indicates the satisfactory performance of the adapted model for any type of wave generation. The numerical model developed under this study can be used for analyzing wave interaction with horizontal slotted submerged porous breakwater having different porosities. Thus the developed model will help the coastal engineers for optimizing the breakwater dimensions during its design.

#### References

- Al-Banna, K. and Liu, P. 2007, Numerical study on the hydraulic performance of submerged porous breakwater under solitary wave attack, *Journal of Coastal Research*, Vol. 50, Pp. 201-205.
- Balaji. R 2012, Performance of Porous Breakwaters: Application of the BOUSS-2D Model, *The Journal of Engineering Research*, Vol. 9, No. 1, Pp. 11-20.
- Brorsen, M and Larsen, J. 1987, Source generation of nonlinear gravity waves with the boundary integral equation method, *Coastal Engineering*, Elsevier, Vol. 11, Pp. 93-113.

## Afroz & Rahman

- Hinatsu, M. 1992, Numerical simulation of unsteady viscous non-linear waves using moving grid system fitted on a free surface. *J. Kansai Soc. Naval Arch. Japan*, Vol. 217, Pp. 1-11
- Ohyama, T. and Nadaoka, K. 1991, Development of a numerical wave tank for analysis of nonlinear and irregular wave field. *Fluid Dynamics Research* Vol. 8, Pp. 231-251
- Rahman, M.A. and Womera, S.A. 2013, Experimental and Numerical Investigation on Wave Interaction with Submerged Breakwater, *Journal of Water Resources and Ocean Science*, Vol. 2, No. 6, Pp. 155-164
- Wu, Y. T., Hsiao, S. C., & Chen, G. S. 2012, Solitary wave interaction with a submerged permeable breakwater: experiment and numerical modeling, *Coastal Engineering Proceedings*, Vol. 1, No. 33, Pp.30.